Earth and Planetary Science Letters, 86 (1987) 327–340
Elsevier Science Publishers B.V., Amsterdam – Printed in The Netherlands

[3]

The southeast Australian lithospheric mantle: isotopic and geochemical constraints on its growth and evolution

William F. McDonough * and Malcolm T. McCulloch

Research School of Earth Sciences, The Australian National University, G.P.O. Box 4, Canberra, A.C.T. 2601 (Australia)

Received June 26, 1986; revised version accepted September 10, 1987

Trace elements and isotopic compositions of whole rocks and mineral separates are reported for 15 spinel-bearing harzburgite and lherzolite xenoliths from southeastern Australia. These samples have an exceedingly large range in isotopic compositions, with $^{87}Sr/^{86}Sr$ ranging from 0.70248 to 0.70834 and ϵ_{Nd} values ranging from +12.7 to −6.3. This range in isotopic compositions can be found in xenoliths from a single locality. The isotopic compositions of clinopyroxene separates and their whole rocks were found to be different in some xenoliths. Samples containing small glass pockets, which replace pre-existing hydrous minerals, generally show only small differences in isotopic composition between clinopyroxene and whole rock. In a modally metasomatized peridotite, significant differences in the Sr and Nd isotopic compositions of a coexisting phlogopite–clinopyroxene pair are present. Coexisting clinopyroxenes and orthopyroxenes from an anhydrous lherzolite have Sr isotopic compositions that are significantly different (0.70248 versus 0.70314), and yield an apparent age of 625 Ma, similar to that found previously by Dasch and Green [1]. However, the Nd isotopic compositions of the clinopyroxene and orthopyroxene are identical indicating recent (within 40 Ma) re-equilibration of Nd.

Sr and Nd concentrations in the whole rocks and clinopyroxenes show an excellent positive correlation, and have an average Sr/Nd ratio of 15. This ratio is similar to the primitive mantle value, as well as that found in primitive MORBs and OIBs, but is much lower than that measured in island arc basalts and what might be predicted for a subduction zone-derived fluid. This indicates that a significant proportion of the Sr and Nd in these peridotites is introduced as a basaltic melt with intraplate chemical characteristics.

The isotopic compositions of the peridotites reflect long-term, small-scale heterogeneities in the continental lithospheric mantle, and are in marked contrast to the near uniform isotopic compositions of the host alkali basalts ($^{87}Sr/^{86}Sr = 0.7038–0.7041$ and $\epsilon_{Nd} = +3.6$ to $+2.9$). A minimum of three evolutionary stages are identified in the growth of the continental lithospheric mantle: an early basalt depletion event, recording the initial development and stabilization of the lithospheric mantle, followed by at least two enrichment episodes. These observations are consistent with continental lithospheric mantle growth involving the underplating of refractory peridotite diapirs.

1. Introduction

The continental lithospheric mantle is that part of the upper mantle below the Mohorovicic discontinuity which is mechanically coupled to the overlying continental crust. Spinel-bearing lherzolite and harzburgite xenoliths brought to the earth's surface by intraplate alkaline basalts provide direct information on the nature of the continental lithosphere. These rocks equilibrated at pressures of about 10–25 kbar and probably represent the major constituent of the continental lithospheric mantle. Mantle xenoliths have been used to identify processes involved in the growth of the continental lithosphere [1–3], constrain the tectonic setting of its formation and provide an estimate of the primitive mantle composition [4]. Additionally, recent studies have proposed that the lithospheric mantle is involved in intraplate basalt genesis [5,6]. Geochemical and isotopic studies of these samples may therefore provide further insights into the composition of the lithospheric mantle as well as melt components derived from it.

There is a basic need for more data which can be used to constrain competing models that describe the formation and growth of the continental

* Current address: Max-Planck-Institut für Chemie, Saarstrasse 23, D-6500, Mainz, F.R.G.

0012-821X/87/$03.50

lithospheric mantle. The models proposed generally involve either underplating of intrinsically buoyant, refractory peridotite diapirs onto the base of the lithosphere during plate-margin and intraplate volcanism [7,9] lithospheric thickening due to post-tectonic, conductive cooling [8,10] or lithospheric doubling due to partial subduction of young oceanic lithosphere [11]. Combined petrological, geochemical and isotopic data gained from detailed studies of these peridotite fragments can therefore offer important constraints for these models.

Chemical and Sr and Nd isotopic results are presented here for a suite of spinel-bearing lherzolite and harzburgite xenoliths from southeast Australia. The data are combined with previous major and trace element studies [1–3] on these and related peridotite samples. We put forth a self-consistent, multistage evolutionary model for the growth and development of the continental lithospheric mantle in southeast Australia and evaluate the role of the lowermost lithosphere in basalt genesis.

2. The samples and previous work

The 15 peridotite xenoliths analyzed in this study come from 7 separate alkine basalt centers in the Pliocene to Recent, Newer volcanics from southeast Australia. The samples are representative of the dominant ultramafic lithology found in the xenolith suites from nearly all of the localities in the field. An effort was made to investigate the most common lithology, the spinel-bearing harzburgite and lherzolite xenoliths. In addition two amphibole-bearing, three phlogopite-bearing samples and several samples which contain glass patches that Frey and Green [2] suggested were melts replacing amphibole and phlogopite were also analysed. Six of these xenoliths are the samples from the classic peridotite study of Frey and Green [2]. Four other samples are from Dasch and Green [1], one sample is from Nickel and Green [3], and the remaining four samples were collected recently. These lherzolite and harzburgite xenoliths all contain, in decreasing order of abundance, olivine, orthopyroxene, clinopyroxene and spinel, and some also contain amphibole, phlogopite or apatite. A Mt. Leura specimen (2642) contains ~ 2% amphibole, whereas the Bullenmerri sample (BM134) contains 4.7% amphibole [3]. Three samples are phlogopite-bearing with modal abundances varying from a trace constituent (2640) to a major component (about 9% in 84438 and 16% in 84413). Apatite has only been identified in one sample (2700) [2]. Small areas of glass, that contain recrystallized olivine and pyroxene, are common to all of the peridotites studies, although abundances of the glass pockets vary from rare to about 0.5% in some samples. Samples are coarse to medium grained, with porphyroclastic textures. Four samples (2730, 2736, BM134 and 85168) are strongly foliated. More detailed petrographic descriptions are given in [1–3]; details of the whole rock and mineral major and trace element chemistry for seven of the xenoliths have been described elsewhere [1–3].

3. Experimental procedures

Whole rock analyses were performed on powders, some of which were used in earlier studies [1–3]. Analyses were performed on 100–250 mg of rock powder. Enclosing basaltic material was removed from the xenolith using a water cooled saw; powders were prepared by extracting centimeter size fragments from coarsely crushed interior material. Up to 40 grams of rock fragments were ground in an agate ringmill for 1 minute. In an attempt to keep sample contamination to a minimum, no additional grinding was performed. Clinopyroxene and phlogopite concentrates were separated from the remaining coarsely crushed fragments. Pure (> 99%) mineral separates were obtained by hand picking, and 50–100 mg aliquots of these separates were used for isotope analyses. An additional experiment was carried out on 4 of these clinopyroxene separates (13–17 mg each) and an orthopyroxene separate (260 mg). Following the technique of Jagoutz [12], the mineral separates were washed for several minutes in warm 5% HF, then warm 2.5*N* HCl, repeatedly rinsed in cold distilled water, and then each mineral grain was examined (using horizontal illumination and a binocular microscope) and those without visible inclusions were selected for analyses. These samples were then leached in a warm (~ 60 °C) ultrasonic bath of 10% HF/2.5*N* HCl for 10 minutes and afterwards rinsed several times in distilled water. All samples

were dissolved in teflon bombs.

The isotopic analyses of whole rocks and some of the clinopyroxene separates (Tables 2 and 3) were carried out on the single collector MSZ mass spectrometer using experimental procedures described previously [6,13] but in contrast to previous work normalized to $^{146}Nd/^{142}Nd = 0.7219$. Additional analyses of ultra-pure clinopyroxene, orthopyroxene and phlogopite separates were determined on a recently acquired MAT-261 multiple-collector mass spectrometer in a static data collection mode. In the latter case Nd isotope analyses involved simultaneous data collection of masses 142, 143, 144, 145, 146, 149 and 150, using mass 149 to monitor Sm interferences, and correcting for mass fractionation by normalizing to $^{146}Nd/^{142}Nd = 0.7219$. Sr isotope analyses involved simultaneous data collection of masses 84, 85, 86, 87 and 88, using mass 85, to monitor Rb interferences, and correcting for mass fractionation by normalizing to $^{86}Sr/^{88}Sr = 0.1194$. Table 1 presents the Sr and Nd isotopic compositions of different standards as measured on the MSZ and MAT-261 mass spectrometers used in this study. Differences expressed as parts in 10^6 in the measured Sr and Nd isotopic compositions of these standards for the two machines are small and relatively constant ($\Delta Sr = 47$ and $\Delta Nd = 37$). The $^{87}Sr/^{86}Sr$ and $^{143}Nd/^{144}Nd$ isotopic compositions of the xenoliths and mineral separates determined using the MSZ have been adjusted using the average Δ values so that they are equivalent to those measured on the MAT 261.

Total chemical blank measured during the analysis period for Nd is $\leqslant 30$ pg, Sm is $\leqslant 10$ pg, Sr is $\leqslant 200$ pg, and Rb is $\leqslant 20$ pg. No correction for procedural blank has been applied. Replicate analyses were performed to evaluate chemical and isotopic variations between separate aliquots of rock powder and to document experimental procedures on samples with low concentrations. Finally, there are significant differences in the $^{87}Rb/^{86}Sr$ and $^{87}Sr/^{86}Sr$ ratios reported in this study and those reported in Dasch and Green [1] for splits of the same sample powders (2730, 2736 and 2769) and the mineral separates (2905).

4. Results

4.1. Whole-rock data

Chemical and isotopic results for whole-rock samples are reported in Table 2. The whole-rock data shows extremely large variation in Sr and Nd isotopic compositions for spinel-bearing lherzolite and harzburgite xenoliths from a given basalt field (Fig. 1). Three samples from Mt. Gambier alone display nearly as large a range in isotopic compositions as found in all of the xenoliths. Combined with earlier isotope data [14] the Mt. Leura peridotites show an enormous variation in Nd isotope composition from $\epsilon_{Nd} = +10.6$ to -7.5. These observations indicate large isotopic heterogeneities in the continental lithospheric mantle beneath southeastern Australia. Moreover, these heterogeneous regions occur even within xenoliths from a single vent and document extreme isotopic

TABLE 1

Sr and Nd isotopic compositions of standards

	MAT-261 mass spectrometer		MSZ mass spectrometer		Δ
Nd standards	$^{143}Nd/^{144}Nd$	*n*	$^{143}Nd/^{144}Nd$	*n*	
BCR-1	0.512653 ± 5	6	0.512608 ± 10	7	+45
BHVO-1	0.512999 ± 5	1	0.512967 ± 17	7	+32
La Jolla	0.511873 ± 5	17	0.511841 ± 7	4	+32
					avg. +37
Sr standards	$^{87}Sr/^{86}Sr$	*n*	$^{87}Sr/^{86}Sr$	n	
BCR-1	0.704960 ± 10	3	0.704988 ± 40	6	−28
E&A	0.707966 ± 15	6	0.708001 ± 12	14	−34
NBS 987	0.710197 ± 4	67	0.710253 ± 25	35	−56
					avg. −47

$\Delta = [(\text{isotope ratio})_{MAT} - (\text{isotope ratio})_{MSZ}] \times 10^6$ Uncertainties reported are $\pm 2\sigma_m$ of the ratios, where n = number of analyses.

TABLE 2

Chemical and isotopic composition of southeast Australian peridotite xenoliths

Locality	Sample	Rb	Sr	$\frac{^{87}Rb}{^{86}Sr}$	$\frac{^{87}Sr}{^{86}Sr}$	Sm	Nd	$\frac{^{147}Sm}{^{144}Nd}$	$\frac{^{143}Nd}{^{144}Nd}$	ϵ_{Nd}	T_{DM}
Anakies	2604	0.144	12.75	0.033	0.70453± 7	0.139	0.848	0.099	0.512654±26	0.1	610
Porndon	84402	0.063	6.298	0.029	0.70464± 5	0.119	0.455	0.158	0.512569±62	−1.6	1340
		0.045	5.762	0.023	0.70463± 4	0.125	0.467	0.162	0.512568±24	−1.6	1430
Leura	2640	0.053	5.054	0.030	0.70482± 4	0.104	0.420	0.150	0.512788±40	2.7	760
Leura	2642	0.042	8.588	0.041	0.70366±20	0.175	0.425	0.249	0.513187±34	10.5	170
		0.051	8.348	0.018	0.70356± 5	0.156	0.386	0.245	0.513176±28	10.3	120
Leura	2769	0.232	11.58	0.058	0.70412± 5	0.203	0.774	0.159	0.512831±18	3.5	760
Leura	85168	0.156	10.73	0.042	0.70383± 3	0.239	0.870	0.166	0.512844±22	3.8	820
Bullenm'	BM134	1.854	53.46	0.100	0.70521± 3	0.701	3.959	0.107	0.512649±20	0.0	660
Noorat	2700	0.371	41.86	0.026	0.70384± 7	0.339	1.805	0.114	0.512686±24	0.7	650
Noorat	84413	36.32	88.61	1.183	0.70546± 3	1.011	5.321	0.119	0.512558±26	−1.8	870
		28.17	90.20	0.903	0.70553± 5	0.975	4.992	0.118	0.512588±24	−1.2	820
		31.84	88.88	1.034	0.70551± 4	1.069	5.493	0.118	0.512560±26	−1.7	850
Shadwell	2669	0.110	23.90	0.013	0.70554± 4	0.282	1.823	0.094	0.512314±24	−6.5	980
Shadwell	84438	22.46	92.30	0.703	0.70505± 3	1.211	5.364	0.137	0.512704±24	1.2	790
Gambier	2728	0.071	7.877	0.026	0.70353±10	0.152	0.441	0.209	0.513118±40	9.2	400
			8.189		0.70334± 4		0.544		0.513099±64	8.8	
		0.066	7.652	0.025	0.70338± 4	0.143	0.424	0.204	0.513108±50	9.0	380
Gambier	2730	0.393	3.373	0.336	0.70834± 4	0.087	0.385	0.136	0.512473±38	−3.4	1180
		0.385	3.366	0.330	0.70830± 4	0.072	0.313	0.140	0.512482±32	−3.2	1210
Gambier	2736	0.201	2.810	0.207	0.70709± 9	0.076	0.331	0.139	0.512426±44	−4.3	1300
		0.205	2.836	0.218	0.70704± 4	0.070	0.296	0.143	0.512418±24	−4.5	1380

Elemental concentrations are given in ppm and have analytical uncertainties of $\leqslant \pm 0.5\%$. Uncertainties in isotope ratios are $\pm 2\sigma_m$ and represent intra-run statistics. All measurements were done on the MSZ mass spectrometer but have been adjusted to be equivalent to those measured on the MAT-261. See Table 1 for information on isotopic standards analyses. ϵ_{Nd} notation as reported in [6] but with $\epsilon_{Nd}(0) = 0.512650$. $T_{DM} = (1/\lambda)\ln\{(^{143}Nd/^{144}Nd_{meas} - ^{143}Nd/^{144}Nd_{DM})/(^{147}Sm/^{144}Nd_{meas} - ^{147}Sm/^{144}Nd_{DM})\}$, where $^{143}Nd/^{144}Nd_{DM} = 0.51316$ and $^{147}Sm/^{144}Nd_{DM} = 0.225$; see [29].

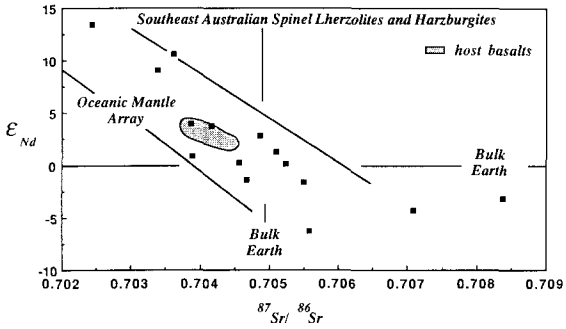

Fig. 1. $^{87}Sr/^{86}Sr$ versus ϵ_{Nd} values for whole rock spinel peridotite xenoliths from southeast Australia. The Sr and Nd isotope composition of the clinopyroxene separate from sample 2905 is plotted here since there was no measured whole rock value. The limits of the oceanic mantle array include ocean islands and MORB [45]. The uncertainty estimate represents a typical 2σ m value. The field of Sr and Nd isotopic compositions for the Newer basalts includes tholeiitic and alkalic basalts [6].

diversity over a restricted vertical section of ~ 40–70 km depth (i.e., the spinel lherzolite field,).

The Sr and Nd isotopic compositions of these peridotites generally plot along the oceanic mantle array (Fig. 1). The large variation in their Sr and Nd isotope compositions is in marked contrast to the limited range in isotope composition of the host alkalic basalts [6]. The spread in isotopic compositions of these peridotites is therefore a feature that cannot be attributed to host basalt contamination. If present, contamination by the host basalts would only reduce the total isotopic variation and thus, the present spread would represent a minimum for the xenolith source region. The two amphibole-bearing and three phlogopite-bearing peridotites have, in general, higher $^{87}Sr/^{86}Sr$ ratios for a given ϵ_{Nd} value compared to the other samples, whereas, the single apatite-

bearing lherzolite plots on the lower left side of the oceanic mantle array.

There is no simple correlation between the Sr and Nd isotopic composition and the presence of a foliated fabric, although two of the four foliated specimens (from Mt. Gambier) have the highest $^{87}Sr/^{86}Sr$ ratios. The high $^{87}Sr/^{86}Sr$ ratios in these two samples are not attributed to secondary surface alteration effects. These samples have high $^{87}Rb/^{86}Sr$ and $^{87}Sr/^{86}Sr$ and low $^{147}Sm/^{144}Nd$ and negative ϵ_{Nd} values, thus reflecting a long-term history of Rb and LREE-enrichment. Both peridotites contain heterogeneously distributed melt pockets which have been interpreted as replacing pre-existing hydrous phases [2]; this interpretation is consistent with their incompatible element enriched character. The Sr and Nd isotopic composition of the foliated Mt. Leura lherzolite, 85168, is not distinct from those of other Mt. Leura peridotites, and is similar to the host alkali basalt isotopic composition. However, it is unlikely that this peridotite has been affected by host basalt contamination since it has very low concentrations of Rb, Sr and the REE compared with the host and has significantly different Rb/Sr and Sm/Nd ratios.

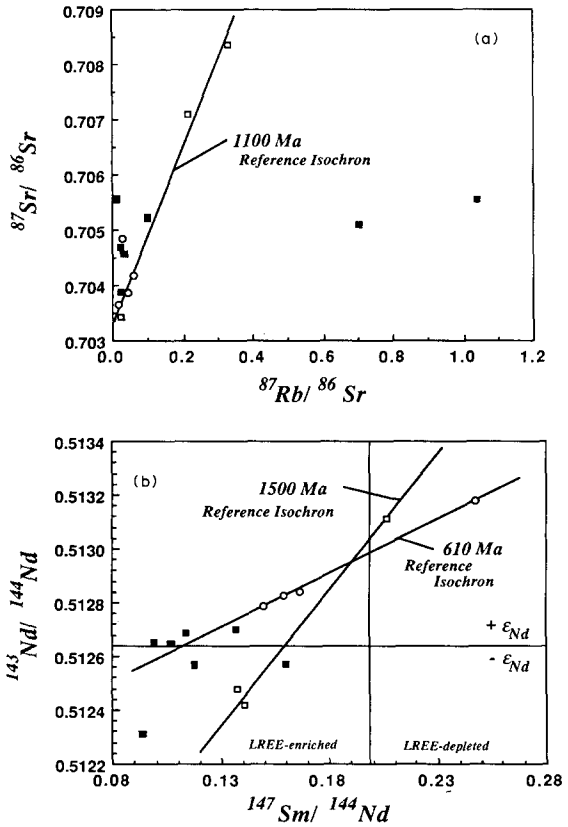

Fig. 2. (a) $^{87}Sr/^{86}Sr$ versus $^{87}Rb/^{86}Sr$ whole rock variation for southeast Australian peridotites. The 1100 Ma reference isochron is shown for the three Mt. Gambier peridotites. Symbols used are, open squares for samples from Mt. Gambier, open circles for samples from Mt. Leura and filled squares for other samples. (b) $^{143}Nd/^{144}Nd$ versus $^{147}Sm/^{144}Nd$ whole rock variation for southeast Australian peridotites. The 1500 Ma reference isochron is shown for the three Mt. Gambier peridotites, and the 610 Ma reference isochron is shown for the four Mt. Leura peridotites, however these ages have no geological significance, see text. The diagram is divided in quadrants based on LREE-depleted versus LREE-enriched patterns and $+\epsilon_{Nd}$ values versus $-\epsilon_{Nd}$ values using primitive mantle values. Symbols as in (a).

Nine out of the fourteen whole rocks studied have positive ϵ_{Nd} values, consistent with a long-term LREE-depleted history (Fig. 2b). However, seven of these nine are LREE-enriched (samples in the upper left quadrant Fig. 2b). This feature has been observed in other peridotite xenolith suites [15–17]. The long-term, LREE-depleted Nd isotopic character is consistent with the peridotite's major and trace element geochemistry which reflect a previous basaltic melt depletion event. Such depleted peridotites were referred to as component A by Frey and Green [2]. Peridotites with LREE-enriched patterns and positive ϵ_{Nd} values must have experienced a recent LREE-enrichment event, although depleted mantle model ages allow this enrichment event to have occurred up to 800 Ma ago (Table 1). This added, LREE-enriched component was called component B by Frey and Green [2] and is present in only some of the depleted peridotites. For example, the Mt. Gambier peridotite (2728) has a near-chondritic REE pattern and a large, positive ϵ_{Nd} value, requiring that at sometime in the past this sample possessed a more LREE-depleted pattern. In contrast, the Mt. Leura peridotite (2642) has a LREE-depleted pattern and a positive ϵ_{Nd} value. It is possible that the amphibole in this sample may be the result of H_2O addition which occurred without significantly changing the bulk rock REE pattern and major element composition.

Fig. 2 gives Rb-Sr(a) and Sm-Nd(b) isochron diagrams for the peridotites. The data plot along highly scattered, positive trends in both diagrams.

The Rb-Sr data for the Mt. Leura samples define a horizontal line with a very large uncertainty. A reference isochron for the Rb-Sr system for the Mt. Gambier peridotites is shown in Fig. 2a and was derived by using the 3 Mt. Gambier samples. The data suggested an age of 1117 ± 69 Ma and an initial $^{87}Sr/^{86}Sr$ of 0.7032. Reference isochrons for the Sm-Nd system are shown for the Mt. Leura and Mt. Gambier peridotites (Fig. 2b). These were generated from a regression for the 4 Mt. Leura peridotites which yielded a 613 ± 96 Ma age with an initial ϵ_{Nd} value of $+6.5$ and 3 Mt. Gambier peridotites which yielded a 1510 ± 525 Ma age with an initial ϵ_{Nd} value of $+7.4$. The different ages determined from the Sr and Nd isotope systems together with the large uncertainties suggest these ages do not have geologic significant.

Differences in absolute concentrations of Sr, Sm and Nd of up to 15% were measured during replicate whole-rock analyses. These differences are attributed to the heterogeneous distribution of clinopyroxene, phlogopite or glass in each aliquot of powder dissolved. This is plausible considering that clinopyroxene, the dominant host for Sr and the REE, commonly constitutes less than 10% by volume of the total rock. The $^{147}Sm/^{144}Nd$ ratios agree at or within $\pm 1\%$ for replicate analyses, although the absolute concentrations differ between each dissolution. Variations in Rb concentrations between replicate analyses may be due to an irregular distribution of Rb along grain boundaries and/or in fluid inclusions [12,18], except in the phlogopite-bearing samples where Rb concentrations will be a function of the amount of phlogopite present in each powder aliquot. Evidence for a grain boundary distribution of Rb can be found by comparing unleached and HF-HCl leached clinopyroxene separates (Table 3). The data show a substantial reduction in the Rb contents and $^{87}Rb/^{86}Sr$ ratios, but no difference in the Sm/Nd ratios or the Sr and Nd isotopic compositions. Chen and Frey [19] also demonstrated that the alkalis are readily removed from acid washed clinopyroxenes in a suite of Mt. Leura peridotite xenoliths, but that the REE and Sr abundances and $^{87}Sr/^{86}Sr$ ratio were unaffected by acid washing. Similarly, in a study of peridotite xenoliths from the southwest United States, Menzies et al. [17] showed that the Sr and Nd isotopic compositions of clinopyroxene separates were within analytical uncertainties before and after HCl leaching experiments.

4.2. Mineral data

The Sr and Nd isotopic compositions of clinopyroxene, orthopyroxene and phlogopite separates are reported in Table 3 together with data for

TABLE 3

Chemical and isotopic compositions of pyroxene and phlogopite separates

Sample	Mineral	Rb	Sr	$\frac{^{87}Rb}{^{86}Sr}$	$\frac{^{87}Sr}{^{86}Sr}$	Sm	Nd	$\frac{^{147}Sm}{^{144}Nd}$	$\frac{^{143}Nd}{^{144}Nd}$	ϵ_{Nd}	T_{DM}
2604	CPX	0.248	498.5	0.0014	0.70448 ± 3	5.406	33.13	0.099	0.512612 ± 20	−0.7	660
	CPX-r	0.299	514.4	0.0017	0.70444 ± 3	6.100	38.00	0.097	0.512644 ± 22	−0.1	620
84402	CPX	0.087	159.0	0.0016	0.70464 ± 5	3.098	11.36	0.165	0.512639 ± 14	−0.2	1320
	CPX-L	0.059	147.3	0.0012	0.70460 ± 2	2.356	8.620	0.165	0.512688 ± 7	0.7	1200
BM-134	CPX	0.116	272.0	0.0012	0.70501 ± 4	1.853	11.55	0.097	0.512625 ± 16	−0.5	640
84413	CPX	1.019	336.1	0.0086	0.70706 ± 4	6.672	32.37	0.125	0.512450 ± 20	−3.9	1080
	CPX-L	0.018	269.5	0.00019	0.70721 ± 2	4.900	24.03	0.123	0.512443 ± 5	−4.0	1070
	phlogopite	200.8	197.3	2.9381	0.70494 ± 4	0.018	0.111	0.096	0.512545 ± 32	−2.0	730
84438	CPX	0.855	214.0	0.0115	0.70530 ± 5	5.418	22.70	0.144	0.512654 ± 20	0.1	950
	CPX-L	0.127	194.6	0.0019	0.70506 ± 2	4.502	18.82	0.145	0.512691 ± 7	0.8	890
2730	CPX	0.348	61.2	0.0164	0.70775 ± 3	1.364	5.813	0.142	0.512598 ± 34	−1.0	1030
2905	CPX-L	0.099	79.72	0.0036	0.70248 ± 1	2.460	5.896	0.252	0.513303 ± 6	12.7	810
	OPX-L	0.0064	0.2383	0.0777	0.70314 ± 1	0.0157	0.0264	0.357	0.513303 ± 20	12.7	170

CPX = clinopyroxene, OPX = orthopyroxene, r = repeat dissolution, L = optically pure and HF-HCl washed separates. CPX-L and OPX-L and phlogopite measured using the MAT 261, all others were done on the MSZ mass spectrometer; see Table 1 for comparison of isotopic standards analyses. Element concentrations are in ppm. See Table 2 for additional details.

leached and unleached mineral separates. In general, the leached and unleached clinopyroxene separates have identical Sr and Nd isotopic compositions, considering uncertainties and differences in machine bias (see Table 1 and discussion in section 3), although in both phlogopite-bearing xenoliths there are relatively small differences in the Sr isotopic compositions which are beyond analytical uncertainties. The $^{87}Sr/^{86}Sr$ ratios of the leached samples are most likely to provide the best estimate of the indigenous clinopyroxene value.

There are slight differences in the Sr and Nd isotopic compositions between clinopyroxene and whole rock analyses for the peridotite 2730, which contains small glass pockets (see [1, fig. 3]). Since no evidence was found for host basalt infiltration [2] we attribute these differences to the influence of the glass phase. These glass pockets are interpreted to be the breakdown products of hydrous phases during decompression in the volcanic pipe [1,2]. Thus, in samples that do not have modal hydrous phases, but do have melt pockets that replace preexisting hydrous phases, the isotopic analyses of clinopyroxene separates alone cannot fully characterize the peridotite xenoliths.

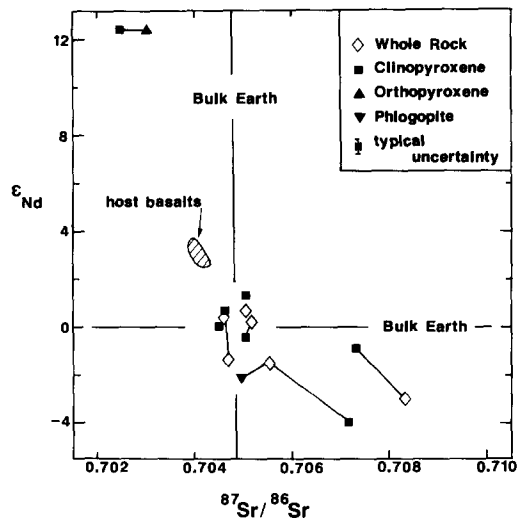

Fig. 3. $^{87}Sr/^{86}Sr$ versus ϵ_{Nd} values for whole rock, clinopyroxene, orthopyroxene and phlogopite mineral separates for peridotite xenoliths from southeast Australia. Orthopyroxene and clinopyroxene for sample 2905 are in equilibrium for Nd but show Sr isotope disequilibrium. The phlogopite and clinopyroxene show both Nd and Sr isotope disequilibrium. The field shown for the 5 host basalts is from McDonough et al. [6]. The error bar indicates the typical $2\sigma_m$ uncertainty.

The mineral phases in the phlogopite lherzolite 84413 show both Nd and Sr isotopic disequilibrium. The $^{143}Nd/^{144}Nd$ ratio of the phlogopite (0.51254 ± 3) is indistinguishable from the whole-rock value (0.51256 ± 3) but higher than the clinopyroxene (0.51244 ± 1). This indicates that the Nd in the phlogopite may have equilibrated with the whole-rock whereas the clinopyroxene has maintained a lower $^{143}Nd/^{144}Nd$ ratio. The $^{87}Sr/^{86}Sr$ ratio of the phlogopite is much lower (0.70498) than that of the clinopyroxene (0.70710-unleached versus 0.70721-leached). The whole-rock has an intermediate $^{87}Sr/^{86}Sr$ value (0.70553). The low $^{87}Sr/^{86}Sr$ of the phlogopite together with its high $^{87}Rb/^{86}Sr$ ratio (2.938) indicates a recent addition of a low $^{87}Sr/^{86}Sr$ component to this rock. For example, it would take about 60 Ma for the phlogopite to evolve to its present $^{87}Sr/^{86}Sr$ value if it was derived from a depleted mantle source (i.e., $^{87}Sr/^{86}Sr = 0.7025$). If the component was derived from a less depleted mantle having a higher $^{87}Sr/^{86}Sr$ ratio, then the age of the phlogopite would be less than 60 Ma. Therefore, phlogopite generation occurred sometime during the Cenozoic, consistent with the presence of the Pliocene to Recent basaltic magmatism in the region. In both phlogopite-bearing samples, the clinoyroxenes have higher $^{87}Sr/^{86}Sr$ ratios than the whole rocks. The balance of the Sr is contained in the phlogopite, which has low $^{87}Sr/^{86}Sr$, thus explaining the differences between clinopyroxene and whole rock values. Phlogopite-bearing peridotites from south Africa have similar isotopic characteristics [20]. Clinopyroxenes in both phlogopite-bearing samples have lower ϵ_{Nd} values than the whole rock, which, in contrast with the Sr system, cannot be explained by the presence of phlogopite since it has both low REE concentrations (less than 0.2 ppm Nd, Table 2) and in the case of sample 84413 an ϵ_{Nd} value which is not distinguishable from the whole-rock value. These differences must be due to the presence of another component. For the phlogite-bearing lherzolite 84413, it is conceiveable that this component represents infiltration by the host basalt, although there is no petrographic evidence for this (see also [2]). Regardless of the explanation, differences in both the Nd and Sr systems

between hydrous and anhydrous phases is indicative of isotopic disequilibrium and suggests recent introduction of a component (e.g., component B of Frey and Green [2]). Additional examples of isotopic disequilibrium have been reported elsewhere (e.g. [15–21,39]).

The clinopyroxene and orthopyroxene separates in sample 2905 have identical Nd isotopic compositions despite differences in $^{147}Sm/^{144}Nd$ ratios, indicating that this peridotite is in Nd isotopic equilibrium. However, considering analytical uncertainties, the maximum age at which this peridotite could have closed to diffusive exchange is 38 Ma ago. This peridotite has a two pyroxene equilibration temperature of about 1030 °C, in agreement with other anhydrous peridotites from the region [2], suggesting it resided at temperatures above Nd closure temperature. In contrast, the Sr isotopic compositions of these coexisting minerals are not the same; the orthopyroxene has a higher $^{87}Sr/^{86}Sr$ ratio (0.70314) than the clinopyroxene (0.70248). This discrepancy between the Sr and Nd isotope systems have been observed before [12,22] and has been attributed to contamination. Dasch and Green [1] found that this sample (2905) preserved a Sr isochron age of about 700 Ma. Interestingly, the Sr isotope data for the clinopyroxene–orthopyroxene pair analysed in this study also yields a 625 Ma age, although the orthopyroxene analysed in this study has a significantly lower $^{87}Sr/^{86}Sr$ ratio than that reported by Dasch and Green (0.70314 compared 0.7060). This suggests that the agreement between the ages may be fortuitous. The apparent Sr age can be attributed to either (1) the $^{87}Sr/^{86}Sr$ composition of the orthopyroxene having been affected by Rb on the grain boundaries, (2) preferential uptake of ^{87}Sr in orthopyroxene versus clinopyroxene, or (3) possibly incomplete purification of mineral separates and/or chemical processing blanks as previously suggested [12,22]. The essentially zero Sm-Nd age also argues against the Rb-Sr age having geologic significance but this may be due to a lower closure temperature for the Nd system compared to Sr. Further studies are necessary in order to better understand the effective grain size of these minerals under mantle conditions and the relative diffusion coefficients of Sr and Nd in natural orthopyroxenes and clinopyroxenes.

5. Discussion

5.1. The nature of the LREE-enriched component

Frey and Green [2] and Nickel and Green [3] suggested that the major and compatible minor element characteristics of these peridotites (their component A) resulted from the extraction of a basaltic melt. This melting event produced residual peridotites which possessed variable depletions in incompatible elements, depending upon the degree of melt extracted. They further suggested that the incompatible minor and trace element compositions of these residual peridotites were increased by the subsequent addition of an added component (their component B), which was enriched in these elements. They argued that component B is genetically unrelated to component A, and represents a liquid derived by a small degree (< 5%) of melting in equilibrium with garnet [2]. This melt was possibly derived from the low velocity zone (LVZ) and interacted with the overlying lithosphere [2]. The nature and origin of this added component has been of considerable interest in recent years [17,28] and is commonly referred to as a metasomatic component. The data presented here allows us to place further constraints on the nature and origin of this component.

The Sr and Nd concentrations in these peridotites are positively correlated (Fig. 4); for $n = 14$, this correlation ($r = 0.985$) corresponds to a > 99.99% level of significance, with an average whole rock Sr/Nd ratio of 14.9 ± 4.0 (1σ). A similar well defined Sr-Nd correlation and relatively constant Sr/Nd ratio (14.5 ± 5.0) is found in clinopyroxene

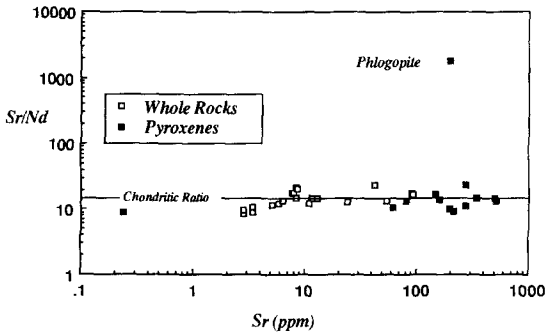

Fig. 4. Sr (ppm) versus Nd (ppm) concentrations for whole rock and their clinopyroxene mineral separates for peridotite xenoliths from southeast Australia. A single phlogopite mineral separate clearly shows a markedly different Sr/Nd ratio.

separates from these peridotites (Fig. 4). In marked contrast, the Sr/Nd ratio of a phlogopite separate is nearly 1800 (Fig. 4), although the Sr/Nd ratios in the phlogopite-bearing peridotites are 17.3. The data indicate an overall control by clinopyroxene on the whole-rock Sr and Nd chemistry, even in the presence of other phases. The average Sr/Nd ratio of these peridotites is similar to the bulk earth Sr/Nd ratio of 17.1 (based on the value for C1 chondrites [23]). In contrast, the Sr/Nd ratio of primitive basalts is dependent upon their tectonic setting. A compilation of Sr and Nd data for relatively unfractionated basalts (e.g., Ni and Cr > 100 ppm, with no evidence of plagioclase fractionation) shows that, in general, MORBs have a low Sr/Nd ratio of 10 to 15, oceanic and continental intraplate basalts have intermediate Sr/Nd ratios of 15 to 20 and island arc basalts have much higher Sr/Nd ratios of 30 to 35 [23-25]. The host Newer basalts have a typical intraplate Sr/Nd ratio of 19.5 [6].

As many of the lherzolites show incompatible element enrichments (e.g. LREE enrichments), it is likely that a significant proportion of the Sr and Nd in the Victorian peridotites was contributed during the enrichment event. If this is true, the Sr/Nd ratios in these peridotites also reflects that of the added component, since none of the modal minerals (except phlogopite) have fractionated Nd from Sr, as evidenced by the similar Sr/Nd ratios between whole rocks and clinopyroxene separates. Thus this enriched component had a Sr/Nd ratio most similar to that of MORB and/or intraplate basalts and is unlike basalts from convergent plate margins or what might be predicted for a fluid flux associated with subduction zone magmatism. The overall incompatible element enrichment produced by the addition of this component suggests it was of an intraplate, rather than MORB character, although a melt component derived by low degrees (< 2%) of melting of the MORB source (i.e., Frey and Green's [2] LVZ source) would have the necessary chemical characteristics. Finally, because the isotopic composition of these peridotites are distinct from their host basalts, the introduced melt component is probably unrelated to this recent intraplate magmatic event.

The above inferences on the tectonic setting and nature of peridotite modification provides an interesting contrast with the tectonic history recorded in the overlying crustal rocks. In this part of southeast Australia there has been an extensive amount of granite genesis in the Paleozoic (~ 400 Ma ago [26]), and a greenstone belt, containing boninites and low-Ti andesites [27], was formed during the Cambrian. Nevertheless, the presence of a subduction zone environment in this region is not recorded in these peridotites.

5.2. Timing of the LREE depletion and enrichment events

The chemical and isotopic compositions of these spinel-bearing lherzolite and harzburgite xenoliths allow formulation of the following model of lithosphere formation and modification. An initially primitive or pyrolitic mantle source underwent partial melting, giving rise to a basaltic melt, and a LREE-depleted residuum. This first stage is envisaged as the initial stabilization of a lithospheric mantle, in conjunction with crust formation. Following this depletion event the Nd isotopic composition of the residuum evolved over some time interval (though not well constrained) to positive ϵ_{Nd} values (or a more positive ϵ_{Nd} value if a depleted mantle model is assumed). Later, LREE-enriched components were introduced into the residuum resulting in a significant decrease in the $^{147}Sm/^{144}Nd$ ratio (< 0.197), and the Nd isotopic composition began evolving to lower ϵ_{Nd} values; in some cases ultimately evolving to negative ϵ_{Nd} values. Using major and trace element data it has been shown [1–3] that each of these peridotites experienced different degrees of depletion and enrichment. The broad range of isotopic compositions found in these peridotites provides additional support for this conclusion.

The considerable scatter of the data on the Sm-Nd and Rb-Sr isochron diagrams (Fig. 2) suggests that these peridotites are mixtures of at least three components. This interpretation is consistent with the data presented here and in previous studies [1–3]. Therefore, these whole-rock samples, and other peridotite samples which show similar geochemical characteristics, will not yield meaningful age information from traditional isochron diagrams. Thus, a previously reported mantle Sr isochron age of 650 Ma derived for a number of peridotite xenoliths from Mt. Leura [28] probably has no age significance, especially in light of the fact that we have been unable to

reproduce these results using samples from the same locality.

There is no unique method for determining the $^{147}Sm/^{144}Nd$ or the $^{143}Nd/^{144}Nd$ of the source prior to the enrichment event, nor can we determine the amount and isotopic composition of the enriched component added to the residual peridotite. Therefore, the precise timing of the depletion or enrichment events cannot be obtained. An approximate estimate of the timing of the LREE enrichments can, however, be made by assuming a simple two stage model, whereby the peridotites experienced one depletion from a chondritic parent, and a latter enrichment event. Estimates for this LREE enrichment event can be calculated using T_{DM} model ages [29] for the most LREE-enriched samples. Such a calculation is justified since these peridotites experienced LREE depletion as a result of basaltic melt extraction. Although the degree of LREE depletion associated with the first event is unknown, it is assumed to be greater than (for small amounts of melt extracted) or equal to that (for larger amounts of melt extracted) of the MORB source. Model ages of LREE-enriched samples are given in Tables 2 and 3 and vary from 600 to 1370 Ma. These models provide only a gross age estimate for the timing of the enrichment event, as they assume only a single-stage enrichment event. These estimates can be significantly in error if the rocks experienced multiple enrichment (or depletion) events. In addition, if the assumed depleted mantle model does not reflect the depletion history of the peridotite, then the uncertainties of these age estimates increase. Furthermore, if these peridotites have experienced multiple enrichment events, then T_{DM} model ages for the most LREE-enriched samples (e.g., 2604 and 2669) represent an upper age limit for the most recent LREE enrichment event. However, for samples 2604 and 2669, this would imply that the last LREE enrichment event was no later than 600 and 970 Ma, respectively. These ages are all significantly older than the Paleozoic plutonism but overlap with the Sm-Nd model ages for the source rocks of these granitoids [13]. This suggests that there is a close relationship between formation of the continental crust and its associated lithospheric mantle.

Like the other samples, the phlogopite-bearing peridotites possess geochemical and isotopic compositions indicating an initial melt depletion and a later incompatible element enrichment (with model ages of ~ 800 Ma). In addition, the low $^{87}Sr/^{86}Sr$ measured for the phlogopite in 84413 suggests that it has also undergone recent addition of a component, post-dating the earlier depletion and enrichment event(s). As discussed previously the Rb-Sr isotopic systematics of the phlogopite indicate a maximum age for its recent component of about 60 Ma consistent with the observation of intraplate magmatism occurred throughout this period [30].

In principle it should also be possible to obtain an approximate estimate of the timing of the initial LREE depletion events. However this is difficult as most of the samples analysed in this study are dominated by the later superimposed LREE enrichment events. Three samples still, however, preserve LREE depletions. These are 2642, 2728 and 2905. The Sm-Nd isotopic analyses of these whole-rock and clinopyroxene separates all give ϵ_{Nd} values that are similar to present-day MORB (ϵ_{Nd} = 9.0 to 12.7). As a consequence they have relatively young T_{DM} model ages of ~ 170 to 400 Ma indicating that relative to a normal MORB source (as given by T_{DM} model evolution) only relatively minor additional depletions have occurred. The timing of the LREE depletion is not well constrained except that it occurred prior to the enrichment events and is therefore > 1000 Ma. It is conceivably that more extensive depletions may have occurred but these have not been preserved due to the later enrichments.

5.3. Evolution of the continental lithospheric mantle

Considerable controversy exists concerning the growth and evolution of continental lithosphere. Growth processes include: magmatic and tectonic accretion during ocean plate subduction, additions to the continental lithosphere during the intracratonic volcanism, and thirdly, additions of lithospheric mantle resulting from the conductive cooling of the lithosphere. A conductive cooling growth model is envisaged as a relatively passive process involving the underplating and thickening of the lithosphere from below as it cools; this growth model has been successfully applied to the oceanic lithosphere and is consistent with geophysical data [9,10,31]. The first two growth

processes are envisaged to be active processes involving significant additions to the lower lithosphere directly from interplate or intraplate magmatism.

The subcrustal lithosphere added to the continents during magmatic events is predicted to be petrologically and chemically distinct from lithospheric mantle added during conductive cooling of the lithosphere. Mantle accreted onto the base of the lithosphere via conductive cooling would presumably have the petrologic, chemical and isotopic characteristics of the convective upper mantle (i.e., the asthenospheric mantle). This mantle would still be capable of producing basaltic melts, possibly with MORB-type compositions. In contrast, mantle accreted during interplate and intraplate magmatism would most likely be depleted peridotite, having a petrologic and chemical composition similar to component A as characterized by Frey and Green [2]. This material would be a Mg-rich, refractory residuum, less dense than the ambient mantle and thus, intrinsically buoyant [8,9,32,33]. The greater the basaltic component (an Fe-rich component) extracted from the peridotite source, the more buoyant the residuum with respect to the surrounding mantle. Such residual peridotite bodies produced during continental magmatism would become permanently trapped beneath the continents and incorporated into the continental lithosphere. In contrast, undepleted or less-depleted peridotite accreted directly onto the lithosphere from the asthenosphere would, because of its higher density, be gravitationally unstable and may sink back into the asthenosphere upon cooling [34,35].

The data gained from the study of these xenoliths provide clues as to the processes involved in the growth and evolution of the continental lithosphere in southeast Australia. The early partial melting event recorded in these peridotite xenoliths documents the initial development and stabilization of the continental lithosphere. This event left the peridotites depleted with respect to a basaltic component and intrinsically buoyant. Thus, the initial growth of the continental lithospheric mantle probably occurred as a result of the underplating of refractory peridotite diapirs, during interplate or intraplate magmatism in this region.

Determining whether the initial lithospheric growth occurred at a convergent plate margin, intraplate setting or spreading plate boundary is not straightforward. Initial lithospheric development has often been envisaged to be in an oceanic spreading ridge environment [1–3, and references therein], although the evidence used to support this is inconclusive. In this respect the constant Sr/Nd ratio in these peridotite xenoliths is significant. If these peridotite bodies were initially emplaced during convergent plate magmatism, then the Sr/Nd ratios in these rocks would reflect those of a subduction-related environment. As already pointed out, the Sr/Nd ratio of 15 ± 4, is consistent with initial lithospheric development in a mid-ocean ridge spreading center (e.g. [1–3]) or an intraplate (possibly rift-type) environment.

Available petrologic, geochemical, isotopic and geophysical data [7–9] support a model in which the continental lithospheric mantle grows through the underplating of buoyancy driven refractory diapirs onto its base. This process leads to the stabilization and development of the continental lithosphere. Other growth processes, such as thermal accretion due to lithospheric cooling, are inferred to be subordinate, and are not supported by petrologic, seismological, thermal, and gravity data [7–9,34,35]. The many constraints provided by these varied approaches indicates that the continental lithospheric mantle is chemically, mechanically and thermally distinct from the underlying convecting upper mantle. Oceanic lithospheric mantle grows over a limited time scale (< 200 Ma) by a combination of active underplating of depleted peridotite as well as by conductive cooling and the passive underplating of asthenosphere. In contrast the continental lithospheric mantle grows over significantly longer time scales by the active underplating of depleted peridotite as well as later enrichment events. Consequently, significant petrologic, geochemical and particularly isotopic differences are expected between the oceanic and continental lithospheric mantles.

Finally, the chemical and isotopic compositions of these peridotite xenoliths show no evidence for a chemically zoned continental lithosphere, contrasting with earlier views [36,37]. Comparisons of chemical and isotopic data for spinel-bearing lherzolite and harzburgite xenoliths with garnet-bearing peridotite xenoliths reveals that both regions of the continental lithosphere are heteroge-

neous, but there is much overlap in their range of compositions [2,3,16,21,38,39]. The fertile, or high temperature, deformed (sheared), garnet peridotites do show chemical and isotopic characteristics which are not found in spinel-bearing peridotite suites, but these may reflect a more prolonged lithospheric history [39].

5.4. Role of the lowermost lithosphere in intraplate volcanism

In recent years, many workers have considered the continental lithospheric mantle as playing an important role in influencing the chemical and isotopic composition of continental basalts. The lithospheric mantle has been suggested to be the source of continental flood basalts [37,40–44], especially in cases where basalts have enriched isotopic characteristics and fairly primitive chemical characteristics. Additionally, recent studies of hotspot related, intraplate oceanic and continental basalts have proposed that melts derived from the lithospheric mantle contribute to hotspot plume-derived melts during basalt genesis [5,6]. In this respect, the chemical and isotopic data gained from the study of peridotite xenolith suites from continental and oceanic environments provides an important constraint on the source reservoirs of intraplate basalts.

We have recently put forth a model for hotspot related intraplate basalt genesis involving the interaction of the lowermost lithosphere and an upwelling hotspot mantle plume [6]. Fig. 5 illustrates the major points of this model for a continental setting. A first-order consideration in this model is the physical consequences resulting from the intrusion of a hot plume of peridotite into the base of the lithosphere. It is likely that the basalt portion of the lithosphere would undergo melting, and that the degree of partial melting would vary considerably over the region of the lithosphere involved. Ultimately, the intraplate basalts which are produced would represent mixtures of plume-derived and lithosphere-derived melt components. It has been argued previously [6] that the lithosphere-derived melt component would dominate the isotopic composition of the alkali basalts, whereas the isotopic composition of the associated tholeiitic basalts would be controlled by the plume-derived melt component.

The broad range of isotopic compositions in

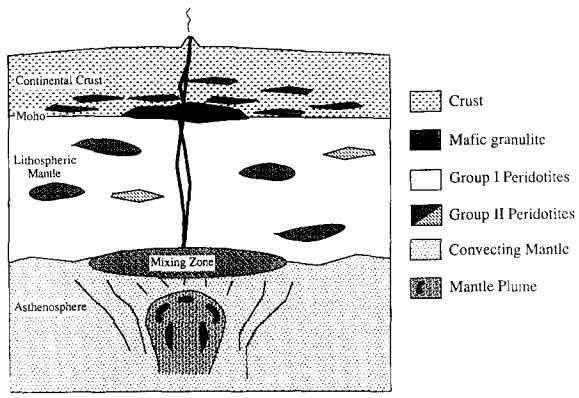

Fig. 5. A mantle model depicting the relative role of the continental lithospheric mantle and an ascending mantle plume during hotspot-related intraplate basalt genesis. In this model a hot ascending mantle plume intrudes the base of the continental lithosphere and initiates melting of the lithospheric mantle; tapped magmas are mixtures of plume-derived and continental lithosphere-derived melt components. Alkalic basalts are considered to be dominated by a continental lithospheric mantle-derived component. As depicted the continental lithospheric mantle contains a diversity of components, possibly of various ages, which are represented by different shadings. Griffin et al. [46] have identified a variety of ultramafic lithologies derived from presumed upper mantle depth from the Bullenmerri and Gnotuk centers in the region.

the southeast Australian peridotites contrasts with the narrow range found in the host basalts [6] indicating that either the source of the alkali basalts is isotopically unlike that of these spinel peridotites or that these basalts are a homogeneous mixture of a similar isotopically diverse lithosphere-derived component. Assuming that the composition of the spinel peridotites is representative of the deeper portion (i.e., the garnet stability field) of the southeast Australian lithosphere, then the alkali basalts could represent homogeneous mixtures of dominantly lithosphere-derived melt components. The homogeneous character of the alkali basalt component is exemplified by four of the host basanite centers, which are separated by more than 50 km, yet have identical Sr, Nd and Pb isotopic compositions [6]. Accordingly, the Sr and Nd isotopic composition of the alkali basalts dominantly reflect an average composition for the continental lithospheric mantle of the region, assuming the melt components are completely homogenized prior to eruption. On this basis the averaged isotopic composition of the lowermost lithosphere in the central portion of the Newer

basalt field is predicted to have a $^{87}Sr/^{86}Sr$ ratio of about 0.7038 and an ϵ_{Nd} value of about +3. Given all the assumptions that are involved it is recognised that this approach provides only a gross compositional estimate. It is noted however that the estimated isotopic composition of this portion of the continental lithosphere lies within the mantle array between the bulk earth and MORB composition, consistent with a long-term history of constant Sr/Nd ratios and multiple episodes of depletion and enrichment events.

Finally, we turn our attention to the possible continental lithospheric mantle sources of continental flood basalts. The large reported range of Sr and Nd isotopic compositions for garnet- and spinel-bearing peridotites [21,39] allows for the possibility that isotopically enriched fragments of the lithospheric mantle may be the source of continental flood basalts. However it is difficult to envision a mechanism whereby continental flood basalts are generated solely by large scale melting of the lithospheric mantle. To raise the lithospheric mantle above its solidus requires a relatively large change in pressure and/or temperature. Continental flood basalts are dominantly tholeiitic or picritic, magmas indicating that large degrees of partial melting are required. Therefore much high temperatures are required for the production of continental flood basalts than alkali basalts indicating that their source is restricted to the hotter regions of the thermal anomaly. Given the need for an external source for the thermal anomaly and that refractory peridotites are common in the continental lithosphere, it is concluded that continental flood basalts are not generated solely from within the lithospheric mantle.

Acknowledgements

We thank Prof. D.H. Green for providing many of the samples investigated in this study as well as introducing M.T.M. to the challenge of resolving the complexities of the southeastern Australian lithosphere. We thank Emil Jagoutz for sharing his expertise on mineral separation techniques and mass spectrometry, and for helping us step up a superior mineral separation techniques. Helpful reviews of earlier versions of this paper were provided by D.H. Green, H.-G. Stosch, F.A. Frey, W.L. Griffin, R.L. Rudnick, C.J. Hawkesworth, J. Hergt, S.O'Reilly and two anonymous reviewers. Fruitful discussions with E. Jagoutz, R.L. Rudnick, H.-G. Stosch, S.-S. Sun and P.K. Zeitler are greatly appreciated.

References

1 E.J. Dasch and D.H. Green, Strontium isotope geochemistry of lherzolite inclusions and host basaltic rocks, Victoria, Australia, Am. J. Sci. 275, 461–469, 1975.
2 F.A. Frey and D.H. Green, The mineralogy, geochemistry and origin of lherzolite inclusions in Victorian basanites, Geochim. Cosmochim. Acta, 38, 1023–1059, 1974.
3 K.G. Nickel and D.H. Green, The nature of the upper-most mantle beneath Victoria, Australia as deduced from ultramafic xenoliths, in: Kimberlites, II. The Mantle and Crust-Mantle Relationships, J. Kornprobst, ed., pp. 161–178, Elsevier, Amsterdam, 1984.
4 E. Jagoutz, H. Palme, H. Baddenhausen, K. Blum, M. Cendales, G. Dreibus, B. Spettel, V. Lorenz and H. Wänke, The abundances of major, minor and trace elements in the Earth's mantle as derived from primitive ultramafic nodules, Proc. 10th Lunar Planet. Sci. Conf., pp. 2013–2050, 1979.
5 C.Y. Chen and F.A. Frey, Trace element and isotopic geochemistry of lavas from Haleakala Volcano, East Maui, Hawaii: implications for the origin of Hawaiian basalts, J. Geophys. Res. 90, 8743–8768, 1985.
6 W.F. McDonough, M.T. McCulloch and S.-S. Sun, Isotopic and geochemical systematics in Tertiary-Recent basalts from southeastern Australia and implications for the evolution of the sub-continental lithosphere, Geochim. Cosmochim. Acta 49, 2051–2067, 1985.
7 E.R. Oxburgh and E.M. Parmentier, Thermal processes in the formation of continental lithosphere, Philos. Trans. R. Soc. London 288, 415–429, 1978.
8 T.H. Jordan, Continents as a chemical boundary layer, Philos. Trans. R. Soc., London 301, 359–373, 1978.
9 A.E. Ringwood, Phase transformations and differentiation in subducted lithosphere: implications for mantle dynamics, basalt petrogenesis, and crustal evolution, J. Geol. 90, 611–643, 1982.
10 S.T. Crough and G.A. Thompson, Thermal model of continental lithosphere, J. Geophys. Res. 81, 4856–4862, 1976.
11 N.J. Vlaar, Thermal anomalies and magmatism due to lithospheric doubling and shifting, Earth Planet. Sci. Lett. 65, 322–330, 1983.
12 E. Jagoutz, R.W. Carlson and G.W. Lugmair, Equilibrated Nd-unequilibrated Sr isotopes in mantle xenoliths, Nature, 286, 708–710, 1980.
13 M.T. McCulloch and B.W. Chappell, Nd isotopic characteristics of S- and I-type granites, Earth Planet. Sci. Lett. 58, 51–64, 1982.
14 C.Y. Chen and F.A. Frey, Multi-stage geochemical events in the upper mantle: evidence from geochemical studies of spinel lherzolites from Mount Leura, Australia, EOS 62, 415, 1981.
15 M. Menzies and V.R. Murthy, Enriched mantle: Nd and Sr isotopes in diopsides from kimberlite nodules, Nature, 283, 634–636, 1980.

16 H.G. Stosch, R.W. Carlson and G.W. Lugmair, Episodic mantle differentiation: Nd and Sr isotopic evidence, Earth Planet. Sci. Lett. 47, 263–271, 1980.
17 M. Menzies, P. Kempton and M. Dungan, Interaction of continental lithosphere and asthenospheric melts below the Geronimo Volcanic Field, Arizona, U.S.A., J. Petrol. 26, 663–693, 1985.
18 A.R. Basu and V.R. Murthy, Ancient lithospheric xenolith in alkali basalt from Baja California, Earth Planet. Sci. Lett. 35, 239–246, 1977.
19 C.Y. Chen and F.A. Frey, Geochemistry of lherzolite inclusions from Mt Leura, Victoria, Australia, EOS 61, 413, 1980.
20 A.J. Erlank, H.L. Allsopp, C.J. Hawkesworth and M. Menzies, Chemical and isotopic characterisation of upper mantle metasomatism in peridotite nodules from the Bulfontein kimberlite, Terra Cognita 2, 261–263, 1982.
21 S. Richardson, A. Erlank and S.R. Hart, Kimberlite-bourne garnet peridotite xenoliths from old enriched subcontinental lithosphere, Earth Planet. Sci. Lett. 75, 116–128, 1985.
22 H.-G. Stosch, G.W. Lugmair and V.I. Kovalenko, Spinel peridotite xenoliths from the Tariat Depression, Mongolia, II. Geochemistry and Sr and Nd isotopic composition and their implications for the evolution of the subcontinental lithosphere, Geochim. Cosmochim. Acta 50, 2601–2614, 1986.
23 S.-S. Sun and W.F. McDonough, Chemical and isotopic systematics of oceanic basalts: implications for mantle composition and processes, in: Magmatism in Ocean Basins, A.D. Saunders and M.J. Norry, eds., Spec. Publ. Geol. Soc. London, in press, 1987.
24 D.J. DePaolo and R.W. Johnson, Magma genesis in the New Britain Island-Arc: constraints from Nd and Sr isotopes and trace-element patterns, Contrib. Mineral. Petrol. 70, 367–379, 1979.
25 J. Gill, Orogenic Andesites and Plate Tectonics, 390 pp., Springer-Verlag, Berlin, 1981.
26 B.W. Chappell, Source rocks of I- and S-type granites in the Lachlan fold belt, southeastern Australia, Philos. Trans. R. Soc. London, Ser. A 310, 693–707, 1984.
27 A.J. Crawford, W.E. Cameron and R.R. Keays, The association boninite low-Ti andesite-tholeiite in the Heathcote Greenstone belt, Victoria; ensimatic setting for the early Lachlan fold belt, Aust. J. Earth Sci. 31, 161–177, 1984.
28 A.R. Burwell, Rb-Sr isotope geochemistry of lherzolites and the constituent minerals from Victoria, Australia, Earth Planet. Sci. Lett. 28, 69–78, 1975.
29 T.C. Liew and M.T. McCulloch, Genesis of granitoid batholiths of Peninsular Malaysia and implications for models of crustal evolution: evidence from a Nd-Sr isotopic and U-Pb zircon study, Geochim. Cosmochim. Acta 49, 587–600, 1985.
30 A. Day, Geochemical constraints on the evolution of magmas and mantle sources beneath southeastern Australia—evidence from Victorian Tertiary lava fields, Geol. Soc. Aust. Abstr. 12, 133–134, 1984.
31 J.G. Sclater, B. Parsons and C. Jaupart, Oceans and continents: similarities and differences in the mechanisms of heat loss, J. Geophys. Res. 86, 11535–11552, 1981.
32 S.P. Clark and A.E. Ringwood, Density distribution and constitution of the mantle, Rev. Geophys. 2, 35–88, 1964.
33 M.J. O'Hara, Is there an Icelandic mantle plume?, Nature 253, 708–710, 1975.
34 G.F. Davies, Thickness and thermal history of continental crust and root zones, Earth Planet. Sci. Lett. 44, 231–238, 1979.
35 G.A. Houseman, D.P. McKenzie and P. Molnar, Convective instability of a thickened boundary layer and its relevance for the thermal evolution of continental convergent belts, J. Geophys. Res. 86(B7), 6115–6132, 1981.
36 C. Brooks, D. James and S.R. Hart, Ancient lithosphere: its role in young continental volcanism, Science 193, 1086–1094, 1976.
37 C.J. Allègre, B. Dupré, P. Richard, D. Rosseau and C. Brooks, Subcontinental versus suboceanic mantle, II. Nd-Sr-Pb isotopic comparison of continental tholeiites with mid-ocean ridge tholeiites, and the structure of the continental lithosphere, Earth Planet. Sci. Lett. 57, 25–34, 1982.
38 P.H. Nixon, N.W. Rogers, I.L. Gibson and A. Grey, Depleted and fertile mantle xenoliths from southern African kimberlites, Annu. Rev. Earth Planet. Sci. 9, 285–309, 1981.
39 M.T. McCulloch, Sm-Nd sysematics in eclogite and garnet peridotite nodules from kimberlites: implications for the early differentiation of the earth, 4th Int. Kimberlite Conf., Geol. Soc. Aust. 16, 285–287, 1986.
40 J. Mahoney, J.D. Macdougall, G.W. Lugmair, A.V. Murali, M. Sankar Das and K. Gopalan, Origin of the Deccan trap flows at Mahabaleshwar inferred from Nd and Sr isotopic and chemical evidence, Earth Planet. Sci. Lett. 60, 47–60, 1982.
41 R.N. Thompson, M.A. Morrison, G.L. Hendry and S.J. Parry, An assessment of the relative roles of crust and mantle in magma genesis: an elemental approach, Philos. Trans. R. Soc. London, Ser. A 310, 549–590, 1984.
42 M.A. Menzies, W.P. Leeman and C.J. Hawkesworth, Geochemical and isotopic evidence for the origin of continental flood basalts with particular reference to the Snake River Plain Idaho, U.S.A., Philos. Trans. R. Soc. London, Ser. A 310, 643–660, 1984.
43 R.W. Carlson, Isotopic constraints on Columbia river flood basalt genesis and the nature of the subcontinental mantle, Geochim. Cosmochim. Acta 48, 2357–2372, 1984.
44 K. Cox and C.J. Hawkesworth, Geochemical stratigraphy of the Deccan Traps at Mahabaleshwar, Western Ghats, India with implications for open system magmatic processes, J. Petrol. 26, 355–377, 1985.
45 W. White, Source of oceanic basalts: Radiogenic isotopic evidence, Geology 13, 115–118, 1985.
46 W. Griffin, S.Y. O'Reilly and J. Hollis, Ultramafic xenoliths from Bullenmerri and Gnotuk Maars, Victoria, Australia: petrology of a sub-continental crust-mantle transition, J. Petrol. 25, 53–87, 1984.